

A One-step Hot-forming Process for the Preparation of Anisotropic Nd-Fe-B Based Magnets

Jung Pil Yang

Research & Development Center, Mando Machinery Corporation
95, Dukso-ri, Wabu-eub, Namyangju-city, Kyongki-do, 472-900 Korea

(Received 30 May 1997)

A new hot-forming process has been studied to produce anisotropic Nd-Fe-B based magnets from melt-spun ribbons. The ribbon fragments were inserted in a Cu tube and hot-deformed together with one-stroke. At a height reduction ratio of 0.44, the melt-spun ribbons were densified into a magnet with a density of 7.14 g/cm^3 , and showed a $(BH)_{\text{max}}$ of 14.6 MGOe. With further deformation, the magnets were plastically deformed with Cu tubes in the lateral direction, and crystallographic anisotropy was introduced. The magnets with a height reduction ratio of 0.75 exhibited magnetic properties of $(BH)_{\text{max}} = 32.1 \text{ MGOe}$, $B_r = 11.7 \text{ kG}$, and $iH_c = 10.6 \text{ kOe}$. This process shows the possibility that the conventional hot-pressing and subsequent die-upsetting for anisotropic magnets can be simplified into a one-step process.

I. Introduction

It is possible to produce anisotropic Nd-Fe-B based magnets of comparable properties both by conventional powder metallurgical method [1] and by melt-spinning and hot-forming methods [2, 3]. Each method has its own advantages and limitations originating from microstructural differences. In the latter method, fully dense anisotropic magnets are usually produced by hot-pressing, and subsequent die-upsetting [3]. The hot-pressing procedure can be characterized by the densification and consolidation of rapidly quenched ribbons into isotropic magnets. To obtain highly anisotropic properties, the hot-pressed magnets should be hot-deformed allowing the lateral plastic flow, i. e., die-upsetted. Although the manufacturing process is complicated by two hot-forming steps, it has been considered to be indispensable for producing the anisotropic magnets with high energy products.

If melt-spun ribbons are densified, and then plastically deformed in the lateral direction with a one-step hot-forming process, anisotropic magnets of high energy product will be produced more readily. In this study, we present a new one-step hot-deformation process using a metal tube for the preparation of anisotropic Nd-Fe-B based magnets [6]. The magnetic properties and microstructures of the hot-formed magnets were also investigated.

II. Experimental Details

The melt-spun ribbons were compacted at room temperature,

and then inserted into a Cu tube. The green magnets and Cu tubes were induction heated to a temperature of $700 \sim 800 \text{ }^\circ\text{C}$, and then compressed to various heights with one-stroke at a cross head speed of 0.2 mm/sec . Fig. 1 shows the schematic diagram of this one-step hot-deformation process. For convenience, the reduction ratio of height e_h was defined as $(h_0-h)/h_0$, where h_0 and h are the height at the original and hot-deformed states, respectively.

The melt-spun ribbons used are Magnequench MQP-A for bonded magnets. The typical magnetic properties at room temperature are given in Table I. Magnetic properties of the hot-worked samples were measured by an integrating fluxmeter. The microstructures were examined by SEM and X-ray diffraction.

Table I. Typical magnetic properties of MQP-A powders at room temperature.

B_r (kG)	iH_c (kOe)	$(BH)_{\text{max}}$ (MGOe)
7.6	15.0	12.0

III. Results and Discussion

Fig. 1 schematically illustrates the concept of the present study. In this process, a Cu tube was employed to introduce the effects of conventional hot-pressing and subsequent die-upsetting processes into a one-step hot-deformation process. Ideally, the densification and texture formation should take place in sequence to maximize the magnetic properties. At the

early stage of deformation, the Cu tube acts as a die in the conventional hot-pressing process and the green compact is densified into a fully dense isotropic magnet.

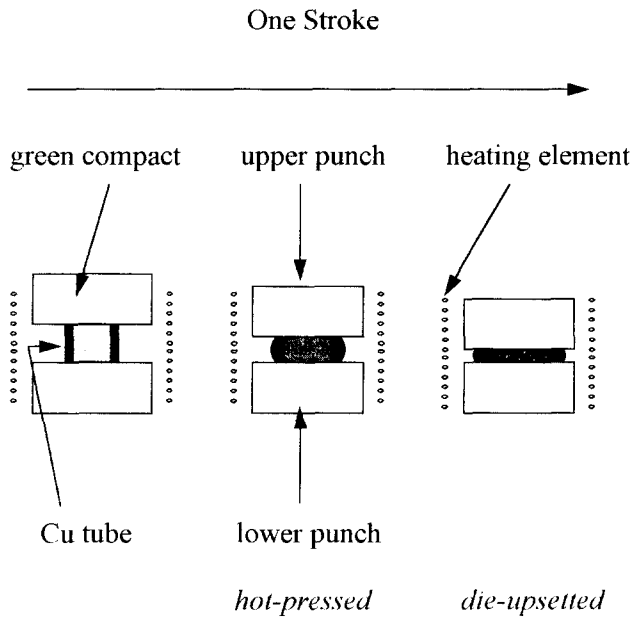


Fig. 1. Schematic diagram showing the one-step hot-deformation process.

As deformation proceeds, the Nd-Fe-B magnet and Cu tube plastically deform in the lateral direction, which introduces the crystallographic texture with a preferred magnetization direction. The magnets undergoing sufficient plastic deformation would exhibit excellent magnetic properties.

As shown in Fig. 2 (a), the tube was designed to minimize the increase in cross-sectional area and buckling of the tube while the tube and green magnet were subjected to hot-deformation. Fig. 2 (b) to (e) are photographs taken from the

hot-deformed samples. The dependence of magnetic properties with the height reduction ratio is shown in Fig. 3. As we increased ϵ_h , the maximum energy product $(BH)_{max}$ and remanence B_r increased, while the intrinsic coercive force iH_c decreased almost linearly.

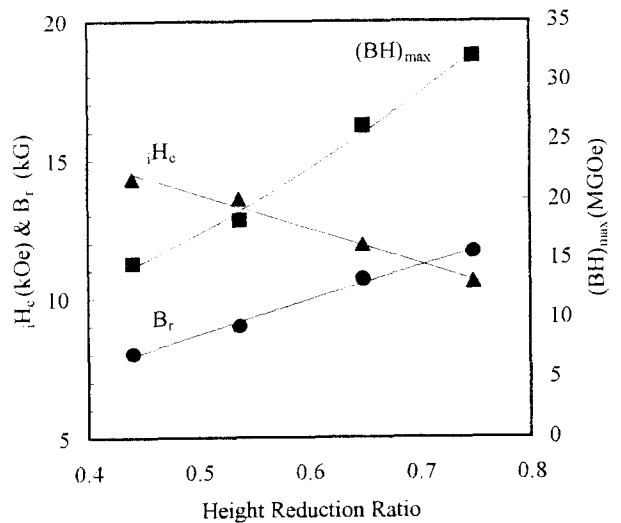


Fig. 3. Variation of magnetic properties with height reduction ratio $((h_0-h)/h_0)$.

When ϵ_h is 0.44, the density of the magnet was 7.14 g/cm^3 , which corresponds to 95 % of the theoretical density of solid $\text{Nd}_2\text{Fe}_{14}\text{B}$. At this stage of deformation, the unique design of the tube makes the increase in diameter negligible compared to the decrease in height. So the compact of melt-spun ribbons with a low density (about 5.2 g/cm^3) was consolidated into a dense magnet. This sample showed a $(BH)_{max}$ of 14.6 MGOe, which is similar to the values of typical hot-pressed magnets.

After the height reduction ratio of 0.44, the density of the magnets is close to 7.5 g/cm^3 . The deformed magnets can be

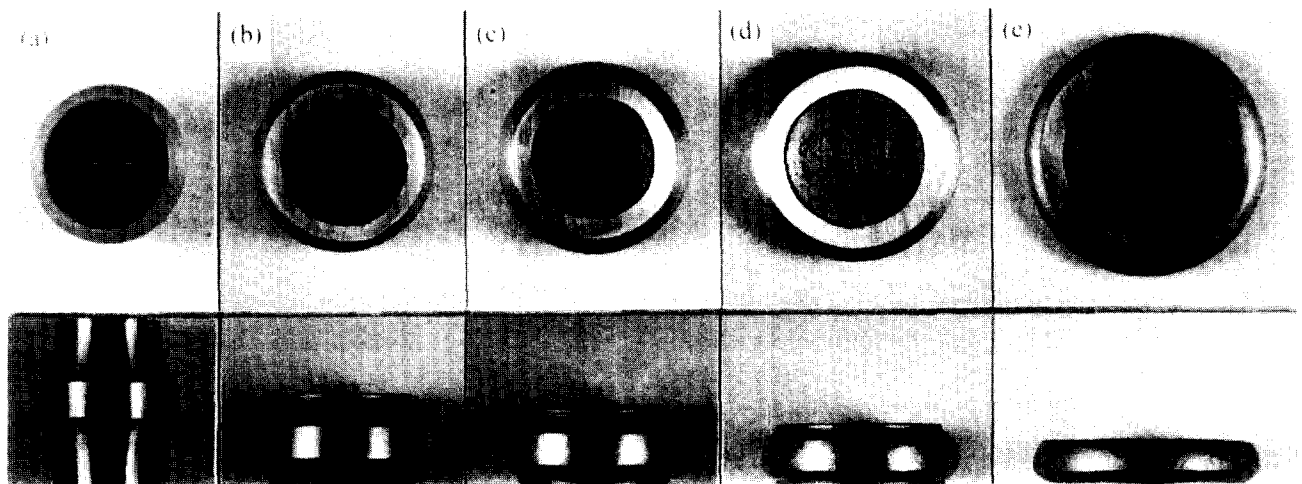


Fig. 2. Photographs of (a) Cu tube, and hot-deformed samples with height reduction ratio of (b) 0.44, (c) 0.54, (d) 0.65, and (e) 0.75.

considered as solid with theoretical density and the volume change is negligible during the hot-forming process. Therefore, the decrease in height directly contributes to the increase in diameter. As e_h reached to 0.65, the value of $(BH)_{max}$ increased to 26.2 MGOe. With further deformation, the $(BH)_{max}$ and B_r increased to 32.1 MGOe and 11.7 kG at a reduction ratio of 0.75, which were comparable to those of die-upsetted magnets. The coercivity values of hot-deformed magnets were relatively lower than those of the hot-pressed and die-upsetted magnets, since the powders used in this study were optimally heat-treated for bonded magnets.

The results of magnetic measurements were consistent with microstructural observations. Fig. 4 shows SEM micrographs taken from the center of fractured surfaces parallel to the press direction. The magnet of $e_h = 0.44$ showed a typical microstructure of hot-pressed magnets [3]. As shown in Fig. 4 (a)~(d), the ribbon fragments became thinner and the interface between the ribbons became less definite. It can be attributed to the fact that the plastic deformation transverse to the press direction was dominant and the ribbon fragments were fused into a dense magnet with increasing e_h . In addition, the one-step hot-forming process accompanied by lateral plastic flow induces magnetic anisotropy.

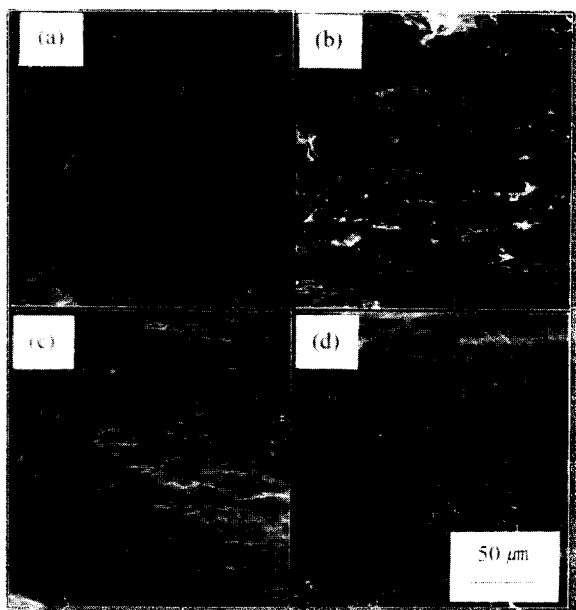


Fig. 4. SEM micrographs taken from the center of the fractured surface of hot-deformed samples with height reduction ratio of (a) 0.44, (b) 0.54, (c) 0.65, and (d) 0.75.

The X-ray spectra taken from the planes normal to the press direction are given in Fig. 5. As shown in Fig. 5 (a) and (b), the intensities of the planes close to the normal direction of crystallographic c -axis, such as (124), (134) and (006), increased by one-step hot press. This result shows good agreement with the previous studies conducted to clarify the mechanism of the

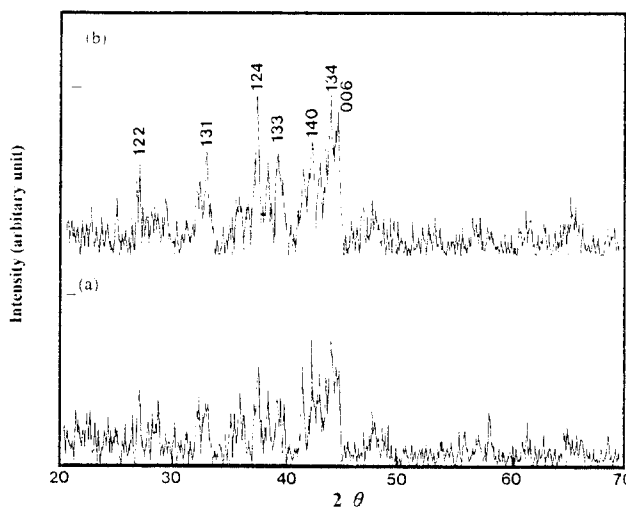


Fig. 5. X-ray spectra taken from the hot-deformed samples with height reduction ratio of (a) 0.44 and (b) 0.75.

texture formation by hot-working [3 ~ 5].

From a practical point of view, it is more desirable to use a cylindrical tube with constant thickness. Fig. 6 shows the macroscopic view of a magnet with a thin-walled Cu tube before and after a one-step hot-deformation. Since the thickness of the cylinder is small compared to the height, the deformation is unstable and buckling of the tube was observed at a relatively low load. When the height reduction ratio is 0.75, a $(BH)_{max}$ of 29.6 MGOe was obtained. The Cu tube and magnet deformed as shown in Fig. 5 due to the symmetric buckling of the tube.

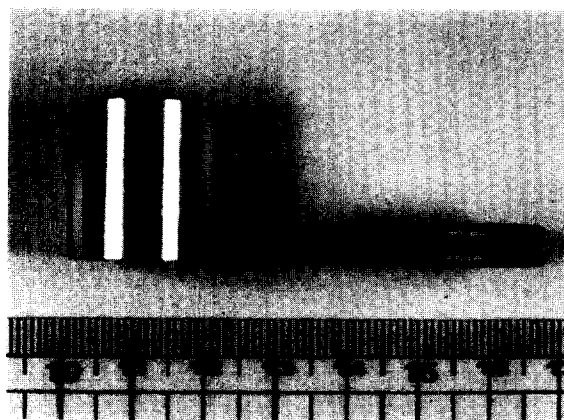


Fig. 6. Photographs of thin-walled cylinder before and after one-step hot-deformation.

The properties of the hot-formed magnets strongly depend on the deformation behavior, which is affected by factors such as mechanical properties and geometry of the tube, hot-forming temperature, and strain rate. The rapidly quenched ribbons deformed in a tube of low carbon steel exhibited a high $(BH)_{max}$ value exceeding 32 MGOe.

In the present study, the tube plays the critical role. At the beginning of deformation, the tube should be strong enough to densify the melt-spun ribbons into a dense magnet. If the magnet density reaches a theoretical value, the tube should be ductile so that the magnetic alignment can be developed by lateral

plastic flow. Therefore, the flow stress and hardenability at deformation temperature should be considered carefully in the material selection and the design of the tube. The deformation of loosely compacted powder and the existence of a liquid phase at the deformation temperature make it difficult to pre-

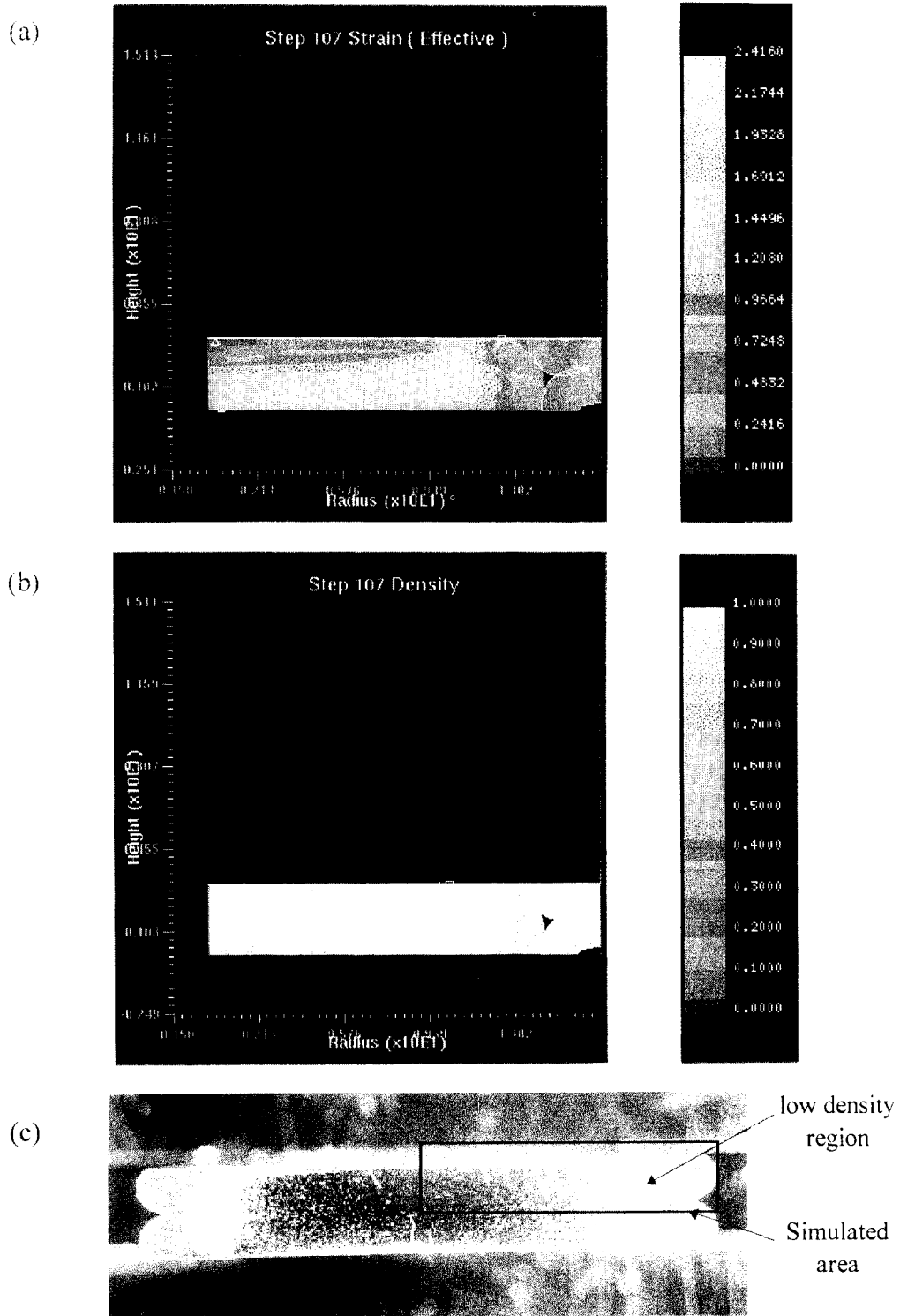


Fig. 7. The simulated distribution of (a) strain, (b) density, and (c) photograph of the cross section of the hot-deformed sample at a height reduction ratio of 0.75.

dict the deformation behavior.

Recently, some computer aided tools can simulate the deformation behavior of powders including the distribution of strain, which is very useful in the optimum design of the tube. Fig. 7 shows the results of the FEM analysis after one-step hot-deformation. The distribution of strain in Fig. 7 (a) reveals that the strain is highest at the center of the hot-deformed specimen, while the strain is low at the regions adjacent to Cu tube and the center of the upper and lower surfaces. The distribution of density follows the same trend as that of strain. The density of magnet is low in the vicinity of Cu tube. The photograph of hot-deformed magnet confirmed the results of simulation (Fig. 7 (c)). The white region adjacent to the Cu tube is porous compared to the other area, and the density is high at the center of the magnet as predicted in Fig. 7 (c).

The magnetic properties of hot-pressed magnets strongly depend on the strain which they undergo during deformation. The actual deformation behavior, such as the distribution of strain and density, well coincided with the FEM analysis. This results also show that the FEM simulation is very useful for the optimum design of tube.

IV. Conclusions

In this study, a new hot-forming method has been studied to produce anisotropic Nd-Fe-B based magnets from melt-spun ribbons. This method using metal tubes simplifies the two hot-

pressing and subsequent die-upsetting processes into one-step hot-forming process. The tubes played the critical role in the development of anisotropic properties. At the early stage of deformation, the tube acted as a hot-pressing die so that the melt-spun ribbons were consolidated into a dense magnet. After the density of magnet increased to a considerable value, the tube was deformed together with magnet, which introduced the magnetic anisotropy while suppressing the formation of surface cracks.

Acknowledgements

The author wish to thank Prof. S. I. Oh, of Seoul National University, for the FEM analysis of hot-forming process.

References

- [1] M. Sagawa, S. Fujimura, N. Togawa, H. Yamamoto, and Y. Matsuura, *J. Appl. Phys.* **55** (6), 2083 (1984).
- [2] J. J. Croat, J. F. Herbst, R. W. Lee, and F. E. Pinkerton, *J. Appl. Phys.* **55** (6), 2078 (1984).
- [3] R. W. Lee, *Appl. Phys. Lett.* **46** (8), 790 (1985).
- [4] Lin Li and C. D. Graham, Jr., *J. Appl. Phys.* **67** (9), 4756 (1990).
- [5] Raja K. Mishra, *J. Appl. Phys.* **62**, 967 (1987).
- [6] Y. B. Kim, C. S. Kim, T. S. Chung and K. S. An, United States Patent No. 5, 516, 371 (1996).